Transition characteristics measured on a 2MW 80m diameter wind turbine rotor in comparison with transition data from wind tunnel measurements

Aagaard Madsen , Helge; Özçakmak, Özge Sinem; Bak, Christian; Troldborg, Niels; Sørensen, Niels N.

Published in:
Proceedings of the AIAA Scitech 2019 Forum

Link to article, DOI:
10.2514/6.2019-0801

Publication date:
2019

Document Version
Publisher's PDF, also known as Version of record

Transition characteristics measured on a 2MW 80m diameter wind turbine rotor in comparison with transition data from wind tunnel measurements

Conference Paper · December 2018

DOI: 10.2514/6.2019-0801

CITATIONS
0

READS
128

6 authors, including:

Helge Aagaard Madsen
Technical University of Denmark
176 PUBLICATIONS **3,049** CITATIONS

SEE PROFILE

Özge Sinem Özçakmak
Technical University of Denmark
4 PUBLICATIONS **0** CITATIONS

SEE PROFILE

Christian Bak
Technical University of Denmark
75 PUBLICATIONS **1,370** CITATIONS

SEE PROFILE

Transition characteristics measured on a 2MW 80m diameter wind turbine rotor in comparison with transition data from wind tunnel measurements

H Aa Madsen* and Ö S Özçakmak† C. Bak‡ N Troldborg§ N N Sørensen¶
DTU Wind Energy, Roskilde, DK 4000, Denmark

J N Sørensen‖
DTU Wind Energy, DTU Lyngby Campus, Niels Koppels Alle 2800 Kgs. Lyngby

One of the main uncertainties in airfoil and rotor design is the determination of the position of transition on the blade as this can have considerable influence on the aerodynamic loads and in particular rotor power. Even for simulations on a rotor in uniform, steady inflow the determination of the position of transition is challenging. The atmospheric inflow on a real MW rotor adds a new level of complexity and uncertainty to the transition modelling and prediction. What is the impact of the atmospheric turbulence on transition compared with transition on a blade section in wind tunnel flow ? The present work is aiming at improving our insight into this subject by analysing transition data measured in the DanAero experiment in 2009 on an industrial 2MW turbine with an 80m rotor with LM38.8 m blades. Transition position is determined from analysing spectra of high frequency (50kHz) surface pressure fluctuations from 56 flush mounted microphones at a radius of 37 m. The position of transition is correlated with measured inflow angle close to the section with transition data. A comparison of the rotor transition with a similar set-up in the LM Glasfiber wind tunnel for transition detection on a 2D blade section copy of the rotor blade, shows a much earlier transition on the pressure side of the rotor blade. On the suction side the difference is much smaller due to an already early transition on the 2D blade section in the wind tunnel, probably caused by small surface irregularities or bumps. Analysing the pressure fluctuations in the laminar boundary layer close to the leading edge which are closely correlated with the turbulent inflow it can be seen that below 300 Hz the energy level on the rotor is much higher than in the tunnel. However, above 300 Hz they are comparable. It is finally shown that the transition on the rotor on the pressure side is moving forward when the spectral energy from 100-300 Hz in the laminar boundary layer increases.

I. Nomenclature

AoA	=	angle of attack
c	=	chord
C_p	=	pressure coefficient
f	=	frequency
f_1	=	lower frequency interval in integration of spectrum
f_2	=	lower frequency interval in integration of spectrum
f_μ	=	The first moment of spectra
K	=	number of windows in the spectral analysis
L_p	=	sound pressure level
L	=	number of pressure samples in window

*Professor, Department of Wind Energy, DTU Risø Campus, Frederiksborgvej 399, DK 4000 Roskilde, Denmark
†PhD student, Department of Wind Energy, DTU Risø Campus, Frederiksborgvej 399, DK 4000 Roskilde, Denmark.
‡Senior researcher, Department of Wind Energy, DTU Risø Campus, Frederiksborgvej 399, DK 4000 Roskilde, Denmark.
§Senior researcher, Department of Wind Energy, DTU Risø Campus, Frederiksborgvej 399, DK 4000 Roskilde, Denmark.
¶Professor, Department of Wind Energy, DTU Risø Campus, Frederiksborgvej 399, DK 4000 Roskilde, Denmark.
‖Professor, DTU Wind Energy, DTU Lyngby Campus Niels Koppels Alle 2800 Kgs. Lyngby, Denmark.

P_{sp} = power spectral density of the surface pressure
R = rotor radius
Re = Reynolds number
x = chordwise position
x_{trp} = transition position on pressure side
x_{trs} = transition position on pressure side
t_k = discrete time at the center of window
TI = turbulence intensity

II. Introduction

The design of new airfoils and wind turbine blades is typically based on computations assuming steady and uniform flow conditions without ambient turbulence. This holds for the code XFOIL which is a common tool for airfoil design but also most CFD computations for airfoil, blade and rotor designs are run with steady inflow, with or without a transition model. A common transition model is the e^n [1] method modelling the growth of Tollmien–Schlichting (TS) waves with the influence of turbulence linked to the n factor. Other transition models like the $\gamma - \tilde{Re}_\theta$ [2] have been tested with promising results on the NREL Phase VI rotor.

However, the inflow conditions on a real rotor operating in the atmospheric boundary layer are highly unsteady, non-uniform and comprising atmospheric turbulence. This is quite different from steady wind tunnel flow with a typical TI below 0.1%. Another difference is also that the wind turbine blade moves with a high speed relative to the mean inflow velocity and almost perpendicular to the main direction of the turbulent inflow.

The fundamental question is if the turbulence level and characteristics of the inflow to the rotor blade section will by-pass the transition mechanism (the amplification of small disturbances) in the e^n method and instead must be modelled with a by-pass transition model [3]. When defining the turbulence level in a wind tunnel it can e.g. be for frequencies above 10 Hz but is it relevant to define the turbulence level for the rotor blade for the same frequency interval ?

Research on transition in atmospheric flow conditions have been carried out within the aeronautical research community. In [4] a comparison of transition characteristics on a small experimental prototype aircraft was carried out with tunnel transition tests of the same wing. A very good correlation was found between the flight and tunnel tests. However, the flights were carried out at 4000 to 10000 ft where the turbulence is much lower than what is present for a wind turbine rotor.

There is thus a need for experimental investigations of the fundamental transition mechanisms on full-scale rotors in atmospheric turbulent inflow in comparison with transition characteristics on airfoils measured under steady flow conditions in wind tunnel tests. The present paper presents and discuss such results obtained in the DanAero projects [5],[6], [7] carried out in collaboration between DTU and the industrial partners LM Glasfiber, Siemens Wind Power, Vestas Wind Systems and the utility company DONG Energy in the period from 2007-2013.

In 2011 the Flensburg University of Applied Sciences [8] carried out a measurement campaign on a 250 kW research turbine with a rotor diameter of 30 m. They showed detection of laminar as well as turbulent boundary layer on the blade using hot film sensors. Further they concluded that because the frequency range of the main energy content of atmospheric flows and wind tunnel flows is strongly different, a TS scenario for transition seemed to be unlikely.

The organization of the present paper is such that first the experimental set-up comprising the full scale rotor experiment and the wind tunnel testing of a 2D blade section with the same cross section geometry as the full scale blade is presented. Then follows a description of the transition detection procedure for the rotor and the wind tunnel blade section. Finally follows a results section and conclusions.

III. Experimental approach

A. The specific experiments from the Danaero project used for the present investigation

In the first DanAero MW project [5],[6] conducted from 2007-2009 a number of coordinated experiments were carried out to provide a comprehensive experimental data basis for studying fundamental aerodynamics and aeroacoustics of MW rotors. The project was followed by the DanAeroII project from 2010-2013 where the data were calibrated and stored into a data base.

For the specific investigation on transition reported in the present paper we use the measurements from two major campaigns in 2009:

1) Measurements of high frequency (50kHz) surface pressure fluctuations and inflow at one radial station, r/R= 0.92 on one of the LM 38.8m blades on the NM80 2 MW turbine at the small Tjæreborg Wind farm in Jutland, Denmark.
2) Measurement in the LM Glasfiber wind tunnel on one airfoil section with exact the same geometry as the blade section at r/R=0.92 on the LM38.8 blade.

However, before going into the details with these measurements we will shortly describe the basic principles in the chosen transition detection method.

B. The basic experimental transition detection method

We chose to base the detection of transition on the analysis of measurements with flush mounted surface microphones of high frequency surface pressure fluctuations in the boundary layer. This method should work for an airfoil section in the wind tunnel as well on a full size wind turbine. It was found that this method probably would be the most robust one. Another important advantage of this method is the ability to provide important insight into aeroacoutic noise generation where the pressure fluctuations in the boundary layer are the main source of both turbulent inflow noise and turbulent trailing edge noise.

The instrumentation and the detection procedures are developed during wind tunnel tests of three different airfoils: NACA0015, B1-18 and C2-18, [9]. The NACA0015 airfoil is well-known whereas the other two are airfoils B1-18 [10] and C2-18 [11] are designed specifically for the outboard part of the blade of a Mega Watt (MW) turbine. These two airfoils are designed to have a considerable part of the boundary layer laminar at low AoA.

The transition detection method is based on tracking the considerable shift in the P_{sp} of the surface pressure fluctuations in the boundary layer when changing from laminar to turbulent flow. This is illustrated in Fig. 1 where the shift in P_{sp} of the microphone signal can be noticed for frequencies above 1-2 kHz for a change in AoA from 7 to 9 deg. However, when the boundary layer is tripped close to the LE and thus turbulent at the 10% chordwise station the same shift is not present as seen on the right graph of Fig. 1. This confirms that the change of P_{sp} integrated over a frequency band from e.g. 1-10 kHz can be used as a good indicator of shift from laminar to turbulent boundary layer.

Details of this procedure are presented in [9] and a comparison of the experimentally derived transition position with Xfoil computations show very good correlation.

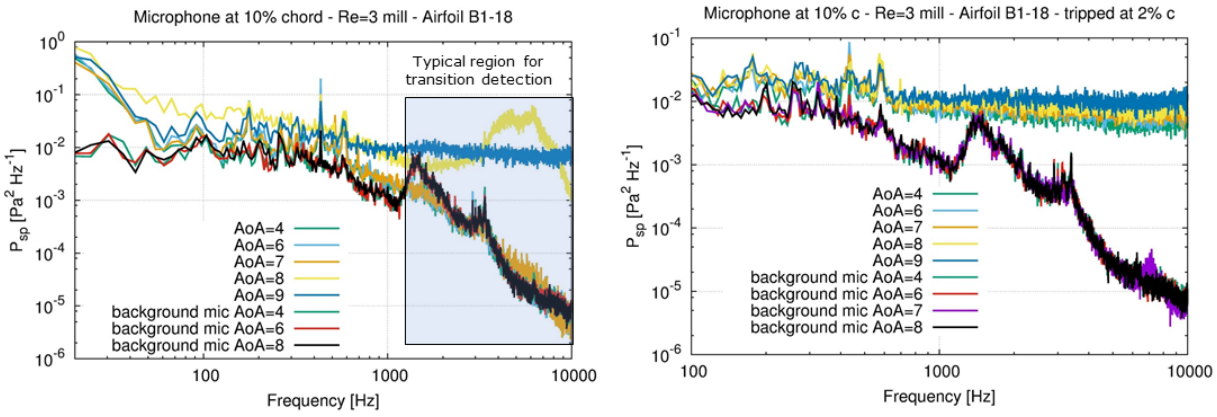

Fig. 1 Left: The P_{sp} of a the signal from a microphone at 10% chord from the LE at different AoA in comparison with the P_{sp} of a background microphone mounted outside on the wind tunnel. Left: Same graphs but now the airfoil is tripped at 2% chord from the LE.

C. Experimental set-up for surface pressure and transition measurements on the 80m diameter NM80 turbine

An overview of the instrumentation of the LM38.8 blade, presented in Table 1 comprises surface pressure and inflow (five hole pitot tubes) measurements at four radial positions. In order to install the surface pressure measurement

equipment and the surface microphones it was necessary to build a complete new blade so that the instruments could be installed during the blade manufacturing process. This was in particular true for the two outboard instrumented sections as these sections could not be accessed after the blade assembling.

A sketch of the blade instrumentation on the test blade is shown in Figure 2 left. It comprises 64 pressure taps at four radial stations, five hole pitot tubes close to these radial positions and finally at the outboard section 56 flush mounted surface microphones. Both the pressure taps and the microphones are pre installed in thin GRP shells that are placed in the mold before the standard blade manufacturing process begins. The microphones are mounted in small aluminium cylindrical houses which are glued into the GRP shells as shown on the sketches and photos in Fig.3. The small cavity between the microphone membrane and the pinhole causes an amplification of the fluctuating pressure due to Helmholtz resonance. A calibration procedure shows a slightly increasing amplification for an increasing frequency peaking at around 4 dB just above 10kHz and then falling quickly off. Finally, the right photo in Fig.3 with the microphones seen from the leading edge shows the the microphones are installed along a line with an angle to the chord. It should also be mentioned that the bugs seen on the blade were not present in the campaign chosen for the present analysis.

Data acquisition is carried out with three different systems as the different type of sensors require different scan rates, Table 1. The slowest system running at 35Hz samples sensors on the turbine and in the nearby meteorology mast. Pressure scanners sample at 200Hz and finally 50kHz is used as sampling rate for the microphones. A common synchronization signal is sampled by all the three systems which allow time aligning the signals in the post processing analysis. In order to limit the amount of data to a manageable size the microphone scanning only runs for a period of 10 sec each one minute.

Table 1 Instrumentation on the LM38.8 blade.

Instrument	Sensor	Position [m]	Sampling rate [Hz]
Strain gauges	Flapwise and edgewise moments	{3.0, 8.0, 13.0, 16.0, 19.0, 22.0, 26.0, 30.0, 34.0, 37.0}	35
Five-hole Pitot tubes	Relative velocity and flow angles	{14.5 20.3, 31.0, 36.0}	35
Pressure taps	Surface pressure	{13.0, 19.0, 30.0, 37.0}	100
Accelerometers	Acceleration	{13.0, 19.0, 30.0, 37.0}	35
Thermometer	Blade temperature	{13.0, 19.0, 30.0, 37.0}	35
Microphones	Surface pressure	37.0	50000

D. The site

The NM80 turbine is located in a small wind farm of eight turbines at the Tjæreborg Enge site in the south western part of Jutland, Denmark. In western direction there is only about 1km to the North Sea so there is a big difference in the characteristics of the inflow to the turbine depending on the wind direction.

The layout of the wind farm is sketched in Fig. 4 which shows the 8 turbines are aligned in two rows. The turbines in the southern row and the instrumented turbine, denoted WT3, are all of the NM80 type, while the others are Vestas V80´s. Being situated in a wind farm the test turbine will be exposed to wake from other turbines for many wind directions. For the present analysis some data are for wake operation caused by WT3 (wind directions from 246 to 266 deg) which is in a distance of 5.9 rotor diameters. Another part of the test campaigns included are for wind directions just below 246 deg.

E. The wind tunnel testing of the blade section copy

In order to investigate the difference in airfoil characteristics and in the present case particularly transition caused by the quite different inflow characteristics on the rotor operating in the atmospheric flow and on an airfoil in wind tunnel flow, a blade section with the measured geometry of the rotor blade cross section at the most outboard radial position, Table 1, is manufactured. The chord and spanwise length of the blade section is 0.9 m and 1.35 m, respectively in order

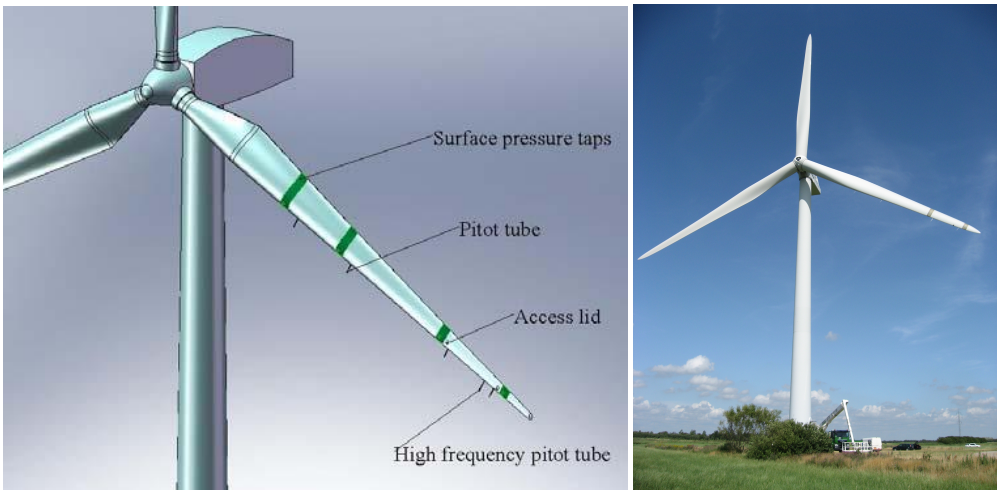

Fig. 2 Left: Sketch showing an overview of the instrumentation of the test blade. Right: The test blade after installation on the turbine in May 2009, replacing one of the original blades.

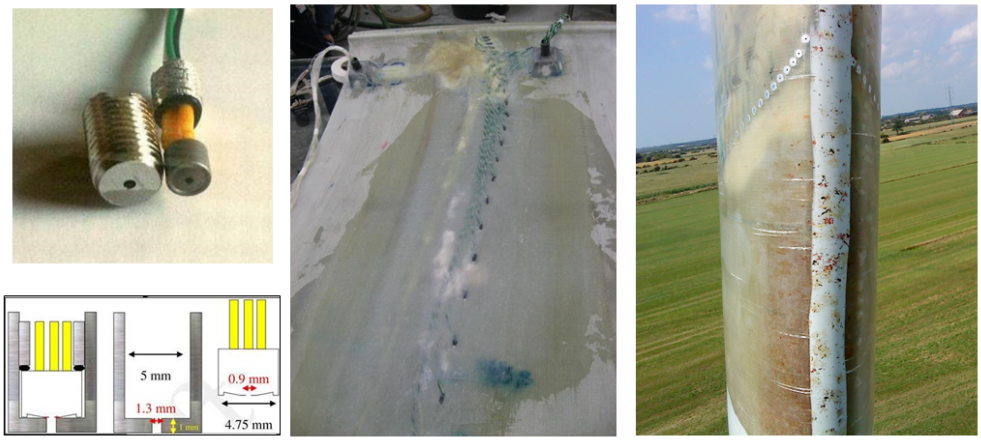

Fig. 3 Left: The Sennheiser KE 4-211-2 microphones are installed in 5 mm diameter cylindrical houses with a pin hole of a diameter of 1.3 mm. Mid: The pressure taps and microphone housings are mounted in a thin GRP shell that as the first step in the blade manufacturing process is laid down in the mold. Right: The microphones on the blade seen from the leading edge. It should be noted that the bugs were not present during the measurements for the data set in the present analysis.

to fit into LM Wind Power wind tunnel. This tunnel is specifically designed for 2D testing of airfoils and has a test section with the dimension of 1.35 m in width, 2.70 m in height, and 7 m in length. The maximum flow speed is 105 m/s and a typical turbulence intensity is 0.1% based on velocity fluctuations above 10 Hz.

The theoretical airfoil contour is the NACA 63-418 airfoil but the actual geometry differs e.g. du to the necessity to have a finite thickness of the trailing edge. However, also the special conditions in manufacturing the test blade where the GRP bands with the pressure taps and microphones are laid down in the mould before the main material of the blade has probably also caused some of the surface irregularities which impacts the surface pressure distributions as will be shown later.

The wind tunnel experiment, the transition detection procedure and the results have been thoroughly described in [12] and will only be summarized here. The blade section was made in an aluminium shell that was sanded as the final step in the manufacturing proces, Fig. 5.

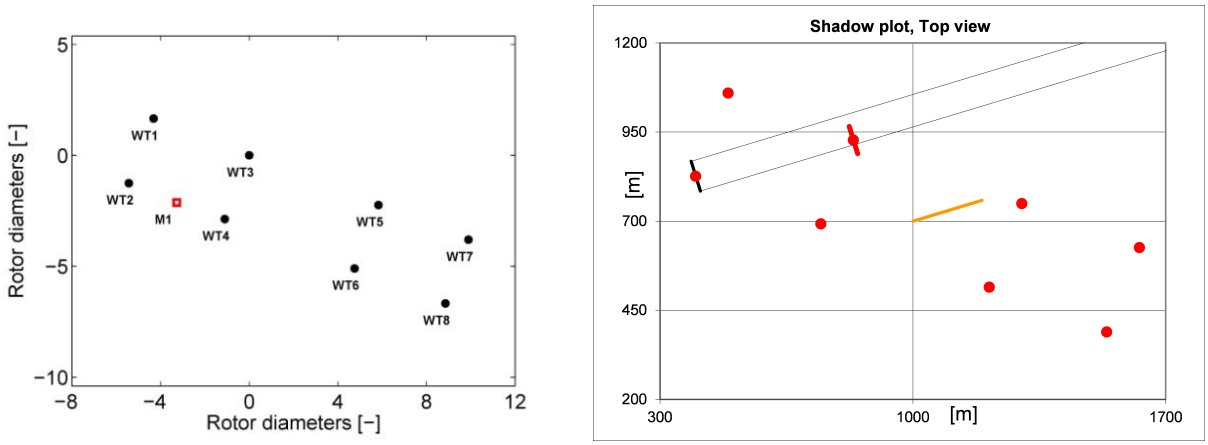

Fig. 4 Left: Figure showing the wind farm layout which consists of eight 80 m diameter turbines in two rows NW - SE. The test turbine is WT3 and SE of the turbine the meteorology mast with a height of 93 m M1 is situated aligned with the turbines in that row. Right: Shadow plot showing the test turbine in wake from upstream turbine for a wind direction of 253 deg which is one of the measurement campaigns included in the present data analysis.

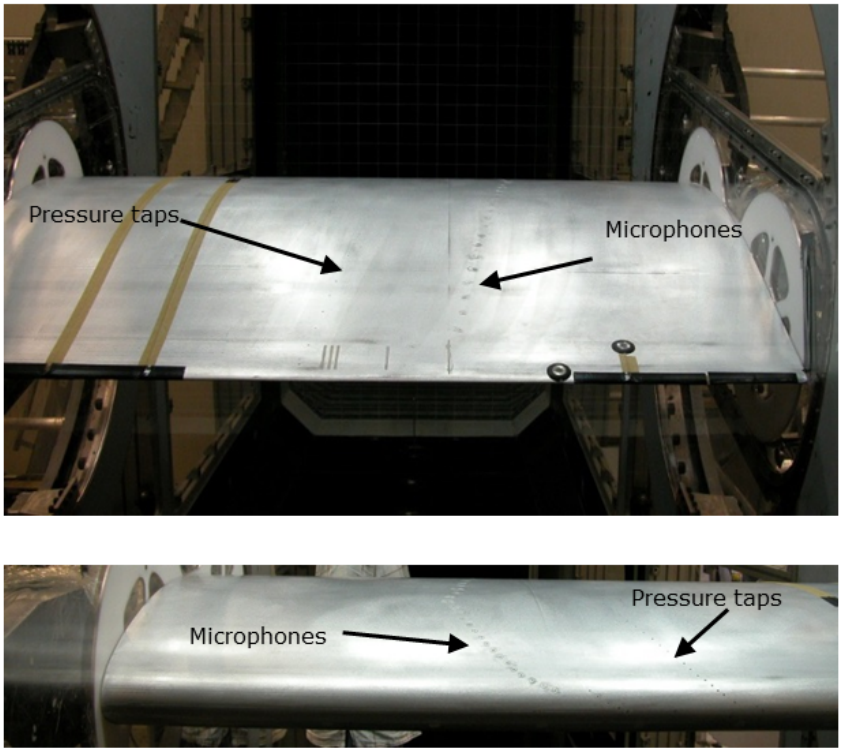

Fig. 5 Upper photo: The 2D blade section installed in the LM wind tunnel seen from the trailing edge towards the leading edge. Lower Photo: Same seen from the leading edge. It should be noted that two surface microphones seen on the upper photo are not used in the present work.

The model is instrumented with 65 pressure taps and 66 microphones distributed on the pressure an suction side, respectively, and in varying span-wise positions in order to minimize the influence on transition by the taps and the

microphone pin holes.

The Experiments are carried out at the Reynolds numbers of ($1.6 \cdot 10^6$, $3 \cdot 10^6$, $4 \cdot 10^6$, $5 \cdot 10^6$ and $6 \cdot 10^6$). The AoA is varied from -15 to 16 deg with one degree increments. Furthermore, the increments are decreased by half between -3 to 5 deg. The microphone data are sampled at 50000 Hz for 10 sec for each test case while the pressures are scanned with 5 Hz for 10 sec.

Measurements are also carried out with different roughness elements and tripping devices on the leading edge. Finally, the influence of adding turbulence to the inflow with two different grids of 100 and 200 mm grid size, respectively, is tested.

IV. Transition detection procedures

As mentioned above the transition detection method is based on tracking the considerable shift in the surface pressure fluctuations in the boundary layer when changing from laminar to turbulent flow. We express the fluctuations by the pressure level L_p and infer transition as locations with a sudden chordwise increase of the L_p.

A. On the rotor

The sound pressure level L_p at each of the 55 microphone positions is computed from the power spectral density of the surface pressure, P_{sp} as follows

$$L_p = 20 \log_{10} \left(\frac{P_{rms}}{p_{ref}} \right) \tag{1}$$

where $p_{ref} = 20 \mu Pa$ and

$$P_{rms}^2 = 2 \int_{f_1}^{f_2} P_{sp}(f) df \tag{2}$$

where $f_1 \leq f \leq f_2$ is a given frequency range.
In order to derive temporal variations in the transition point, each time series (all 10sec long) of surface pressure measurements are divided into K sections (windows) with a 50% overlap and for each of these windows L_p is computed from Eq. 1 and 2. To each of the K windows is then associated a sound pressure level $L_{p,k}$ and a discrete time t_k, which is taken to be at the center of the window.

The number of surface pressure samples in each window is denoted L, which is equivalent to a time span of $\Delta t = L/f_s$, where $f_s = 50\ kHz$ is the sampling frequency.

1. Detection of transition summarized

The transition point at each discrete time step t_k is determined from the chordwise distribution of the sound pressure level, L_p in the following way:

- Sort L_p according to chordwise position, x, of the 55 microphones.
- Filter spatially L_p to obtain a smooth distribution denoted $L_p(x)$.
- Determine transition points, x_t, as positions where the chordwise derivative of $L_p(x)$ is larger than a specified limit $(dL_p(x)/dx)_{limit}$.
- In general there will be a range of chordwise positions which fulfils this criteria and the exact position is defined to be the zero crossing of the second order derivative $d^2L_p(x)/dx^2$.
- If more than two chordwise positions on each side of the airfoil satisfy the criteria then $(dL_p(x)/dx)_{limit}$ is increased until only two transition points are found on each side of the airfoil.

Figure 6 shows an example of calculated transition points together with the corresponding sound pressure level and its first and second derivative. The reason that often two transition positions are found is probably partly due to surface irregularities causing transition and relaminarization. The parameters used in Figure 6 are: $(dL_p(x)/dx)_{limit} = 350\ dB$, f_1 = 2.0 kHz, f_2 = 6.0 kHz and $L = 2048$. See [13] and [7] for more details.

B. Wind tunnel testing

The main differences for detection of transition in the wind tunnel compared with the rotor data above are that the conditions are much more steady and that the frequency content at lower frequencies (e.g. below 500 Hz) is much lower.

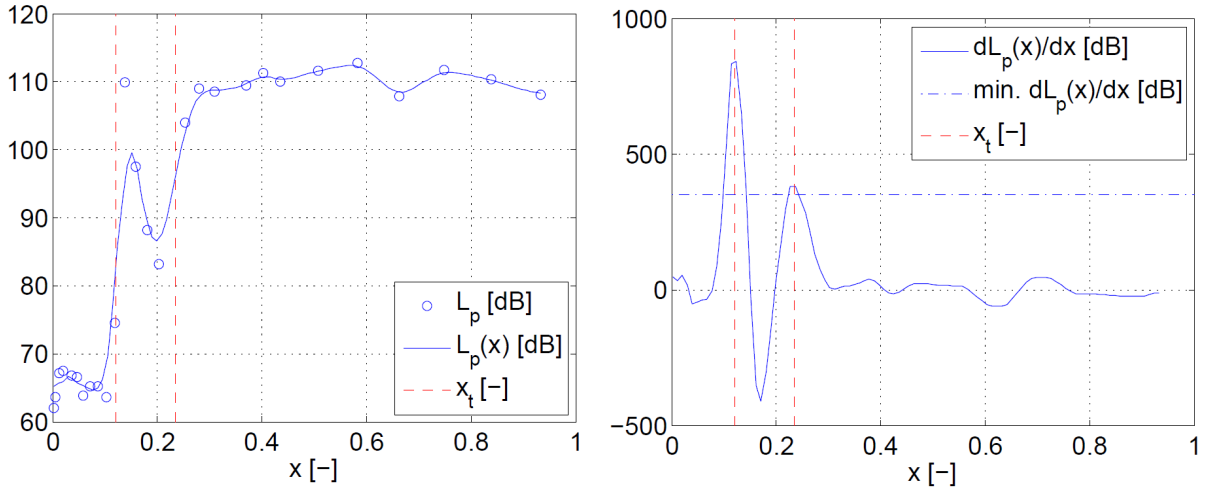

Fig. 6 Example of calculated transition points on suctions side at a given time t_k and the corresponding SPL (a) as well as its derivative (b) and second derivative. Figure from [13].

It means that a method based on the first moment of spectra as discussed in [12] seems to be slightly more precise than the above method.

The first moment f_μ is calculated by Equation 3:

$$f_\mu = \frac{\int_{f_1}^{f_2} f \cdot P_{sp}\, df}{\int_{f_1}^{f_2} P_{sp}\, df} \tag{3}$$

According to the moment method, maximum positive derivative of f_μ with respect to chordwise position gives the transition location for each angle of attack value as shown in Equation 4:

$$x_{tr} = x \rightarrow \quad max(\frac{df_\mu}{dx}). \tag{4}$$

See [12] for comparison of the two detection procedures. The wind tunnel transition results in the present paper are based on the moment method and it should also be noted that a frequency interval from 2 to 7 kHz was used in the integration of the spectra for the wind tunnel.

V. Results

A. The selected time series

In the present paper the focus of the data analysis is on measurement campaigns from the beginning of the total test period of about 2½ months. The test turbine was in operation first time on June 26, 2009 and the two data sets chosen are from July 16th and 21st. The blade is thus still clean as the turbine was only in operation during the specific test campaigns. Later the blade was hit by bugs as can be seen on the photo in Fig. 3.

On the 16th of July the wind speed was around 6 m/s at hub height with a mean wind direction between 242-248 deg which means just outside the wake of WT2, Fig. 4. In the other campaign from the 21st of July the mean wind speed is slightly higher, between 6 to 7 m/s but as the turbine most of the time is in partial or full wake of WT3 due to wind directions between 253 to 257 deg, the effective wind speed is lower. In the selected periods the rotational speed of the rotor is almost constant and close to 16 rpm.

B. Time series of transition, inflow and binned pressure distributions

We show first time series of AoA and transition for three different inflow situations together with binned pressure distributions on blade azimuth, Fig. 7.

Unfortunately the two outboard five hole pitot tubes are not in operation during these campaigns. One option is to use a third pitot tube at radius 20.3 m which means about 16.7 m from the cross section with the microphones and pressure taps. However with considerable variation of the inflow over the rotor disc as for example in partial wake this would introduce a considerable uncertainty. We derived therefore an alternative AoA^* based on the aerodynamic

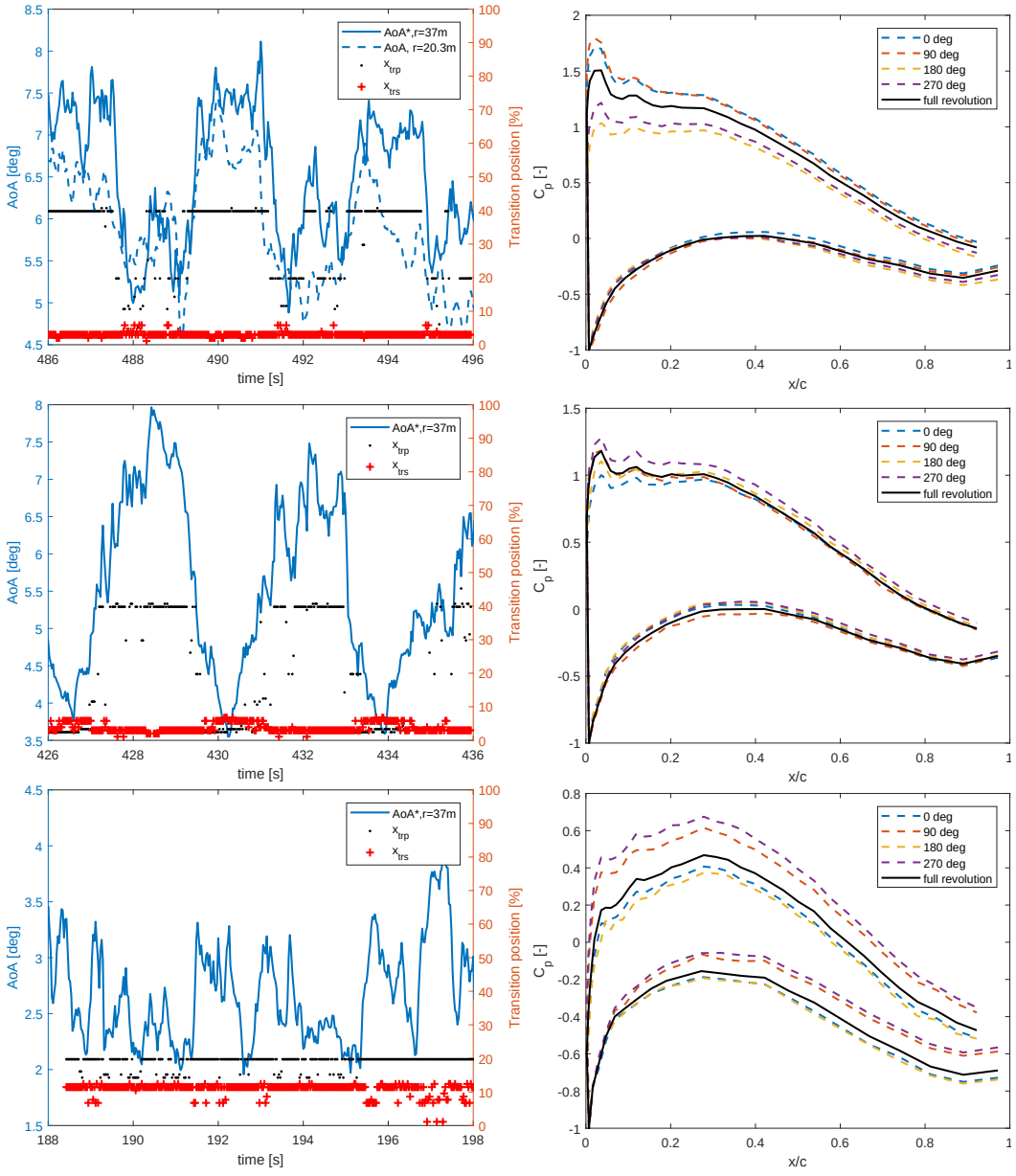

Fig. 7 Upper: Left graph showing inflow measurements (AoA from the five hole pitot at radius 20.3 m and AoA^* derived from aerodynamic force f_y perpendicular to the chord) and transition on suction and pressure side of the blade for a 10 sec period for operation in half wake. Right graph showing measured pressure distribution for the same period for the blade in four azimuth positions (0 deg blade vertical upwards). Middle: Same plots for a narrow wake. Bottom: Same plots but for free inflow.

normal force to the chord at this radial position integrated from the pressure distribution. The link from aerodynamic force to AoA is derived with the aerelastic code HAWC2 [14] developed by DTU.

On the upper left graph we show both $AoA's$. Part of the time they are close to each other but deviate in other periods due to difference in inflow over a span of 16.7 m. The AoA variations are typical for a half wake operation. It means that the AoA is high when the blade passes through the free inflow and then decreases considerably when entering the wake with a velocity deficit. In the centre of the wake the velocity deficit is often slightly less pronounced as also seen here around time 489 sec which is due to lower local thrust on the inboard part of the rotor. Variations between 5 to 8 deg are seen.

The transition on the pressure side is stabilizing around 40% when the AoA is high and then moves close to the LE when the AoA is low. On the suction side, the transition is close to the LE and only moves slightly when the AoA is low.

For supporting the interpretation of the transition, we show in Fig. 7 (right) the measured pressure distribution at the nearby pressure taps. The pressure data are binned on an azimuth interval of 10 deg around the four azimuth positions; 0 deg which is blade up and then 90, 180 and 270 deg, respectively. The variation between the four pressure distributions are thus due to the variation of AoA over one rotor revolution.

On the suction side, a small bump in the pressure distribution is seen, caused by a small bump in the surface geometry. As mentioned earlier this is probably due to the special manufacturing approach that is used for the test blade to build in the measurement equipment. Smaller bumps can be seen further downstream on the suction side whereas the pressure distributions on the pressure side are quite smooth.

The middle graphs on Fig. 7 show the same type of results as described above but for a half wake situation that results in slightly bigger AoA amplitudes. Again at the lowest AoA the x_{trs} moves away from the LE but indicates less than 10% laminar flow.

The AoA variations in the lower left graph for the turbine operating in free inflow are much less and a maximum amplitude of 1.5 deg is seen. This results in an almost stable x_{trp} of 20% and x_{trs} of 10 to 12%. Although the pressure gradient on the suction side is now favourable up to about 30% the x_{trs} is close to the LE. The earlier transition is probably cause by the the small bumps in the pressure distribution.

C. Rotor transition compared with transition on the blade section in the LM wind tunnel

The total transition analysis is based on three 10 min time series for partial and full wake operation from the 21st of July and likewise three 10 min series from 16th of July with free inflow. With the microphones scanned over 10 sec period each minute this gives a total data base of thirty 10 sec time series for transition detection. Actually it is slightly less as a few series are not included due to low rotational speed of the turbine.

The x_{trp} is shown on the upper graph of Fig. 8 in comparison with the results from wind tunnel testing at Re 5 mill on the similar 2D airfoil section model as presented in [12]. A considerable shift of x_{trp} towards higher AoA is seen which amounts to 8 to 10 deg when x_{trp} is close to the LE. However, the deviation almost disappears when the transition is around mid chord. It also appears that the transition for the wake operation is shifted more than the one for free inflow.

The lower graph in Fig. 8 shows the comparison of rotor vs. wind tunnel transition results for the suction side. Again the wind tunnel results are from [12] where it was found that the transition was shifted towards lower AoA than e.g predictions by Xfoil indicated. The causes were also discussed and a combination of interaction from neighbouring/upstream microphones and the surface irregularities were mentioned as possible effects.

Comparing with the rotor transition for the suction side we see here a much closer correlation than for the pressure side with only a small shift towards lower AoA (earlier transition) than in the wind tunnel testing.

D. Possible causes of the differences between wind tunnel and rotor transition

The experimental set-up is designed to enable as close as possible comparison of the transition on the rotor and in the wind tunnel. Most important is that the blade section for the wind tunnel testing is manufactured with the same surface geometry as measured on the rotor. It means also that the same surface irregularities/bumps are present on the wind tunnel model and probably have a considerable impact on enforcing an earlier transition as compared with a completely smooth model. However, for the pressure side the transition measured on the pressure in the wind tunnel correlated well with Xfoil predictions [12].

We will therefore focus our discussion on the causes of the considerable deviations between transition characteristics found on the pressure side and in particular look into the differences in inflow to the blade section on the rotor and in the wind tunnel.

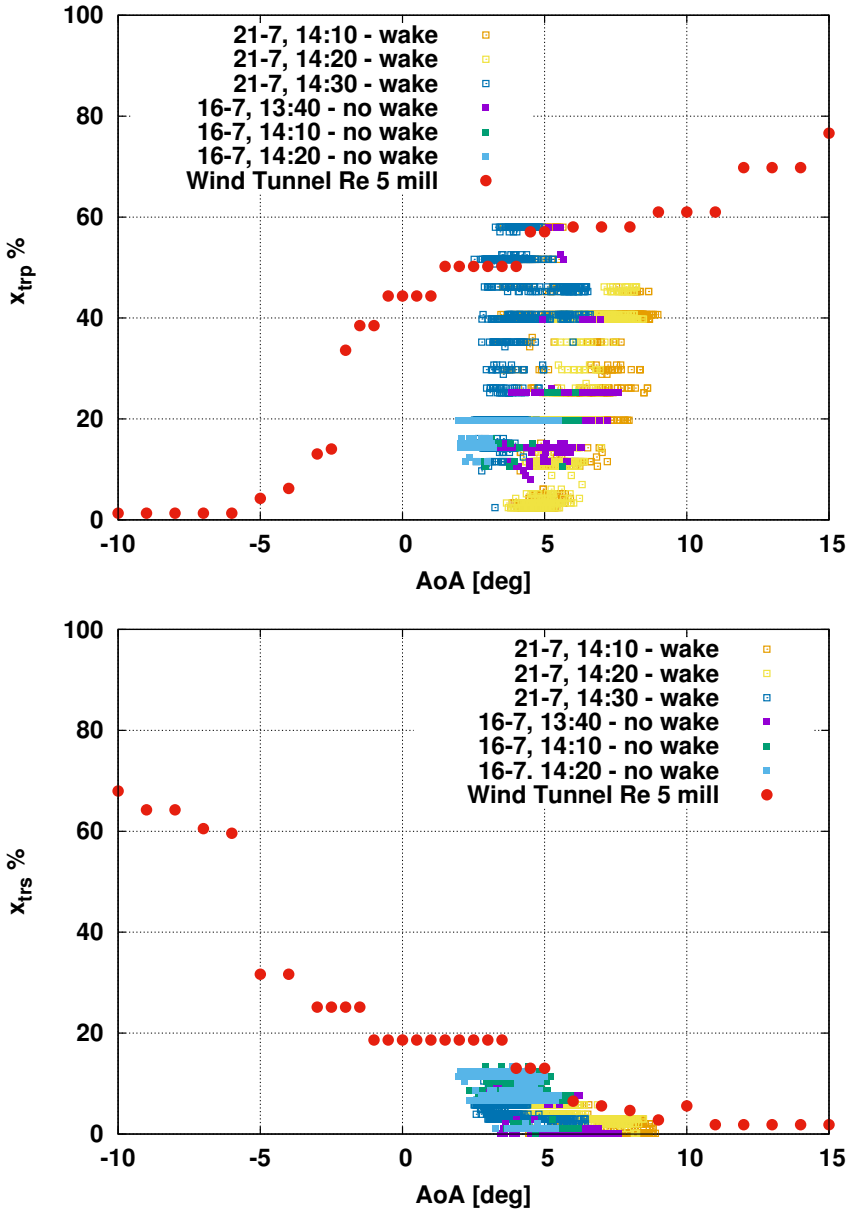

Fig. 8 Upper: Derived transition on the pressure side for the rotor in comparison with wind tunnel measurents at Re 5mill. Lower: Same for the suction side.

E. Differences inflow characteristics between wind tunnel and rotor

We use the power spectra of the microphone signal close to the leading edge (0.2%) on the suction side as basis for discussion of the inflow characteristics. At the 0.2% position the boundary layer is laminar and the spectral characteristics for the pressure fluctuation in the boundary layer are closely linked to the inflow turbulence characteristics as e.g. used in turbulent inflow noise modelling [15].

The power spectra for different flow condition in the wind tunnel and on the rotor are shown in Fig. 9. For the rotor the spectra are based on the whole 10 sec long time series but keeping in mind that considerable variations will occur over the 10 sec. Two arbitrarily selected cases for wake inflow and free inflow, respectively, are shown. It can be seen that the spectra for wake inflow are slightly higher than for the free inflow. This is expected for low frequencies where it is known that in wake operation the atmospheric inflow turbulence can be almost doubled compared with free inflow

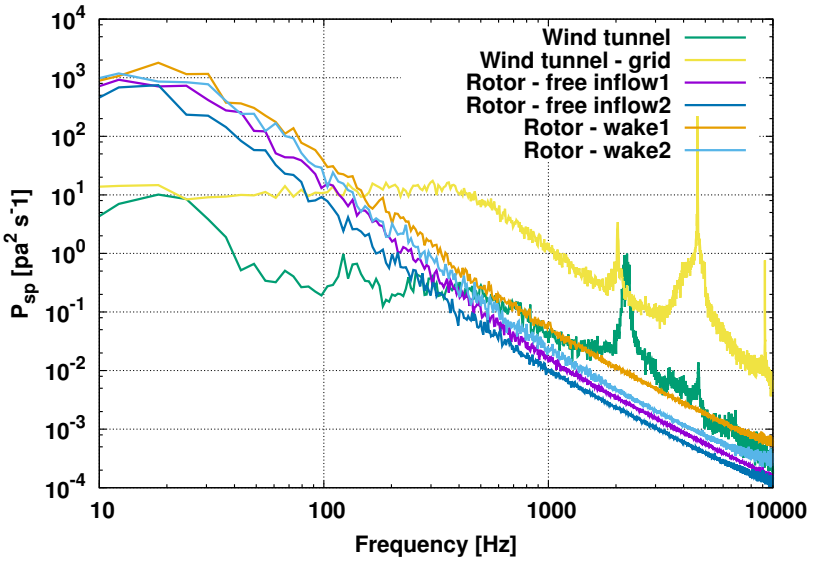

Fig. 9 The power spectra of the signal from the microphone on the suction side at 0.2% chord from the LE at a Re 4 mill and an AoA of 5 deg in the wind tunnel cases and the same mean AoA for the rotor cases but with considerable variations over the 10 sec. Two arbitrary selected cases, 1 and 2 for the rotor in free inflow and wake operation, respectively are shown. The cases from the wind tunnel are for a flow velocity of 66.7 m/s (Re 4 mill) with free inflow and with a grid with size 100mm x 100 mm in the inlet to the test section. In order to compensate for the lower inflow relative velocity on the rotor (about $62m/s$) the wind tunnel spectra are downscaled with a factor $(66.7/62)^6 = 0.64$. The v^6 scaling of the spectra of the pressure fluctuations was confirmed by comparing spectra in the wind tunnel measured at Re 4 and 5 mill, respectively.

conditions.

Comparing now with the spectrum for the wind tunnel blade section (no grid) it is seen that the spectral energy for the rotor is much higher up to about 300 Hz. Above 300 Hz the wind tunnel spectrum follow the upper curve (wake operation) from the rotor measurements. It should be mentioned that the turbulence intensity in the LM wind tunnel based on frequencies above 10 Hz has been measured to about 0.1% [15].

Measurements in the wind tunnel were also conducted with a grid of 100 mm x 100 mm inserted in the inlet. This increases the spectrum for frequencies higher than 100 to 200 Hz considerably above the rotor spectra.

The time variation of the spectra of L_p on the rotor are further explored by generating the water fall plots for different frequency intervals shown in Fig. 10. For the frequency band from 100 to 300 Hz shown in the upper left graph, we can see some high energy regions close to the LE (e.g. within 1-2%) which means pressure fluctuations in the laminar boundary layer caused by the turbulent inflow. Qualitatively there seems also to be a correlation with the transition position which is based on the frequency interval used in the lower right plot of Fig. 10. When the energy is high in the 100-300 Hz band close to the LE, the transition is close to the LE as seen in the lower right graph.

F. Impact on transition from the 100 to 300 Hz spectrum at the LE

The observations above based on the spectra in Fig. 9 and Fig. 10 led to an investigation of a possible impact of the spectral energy in the 100 to 300 Hz interval for a position close to the LE and movement of transition for a fixed AoA. The result is shown in Fig. 11 where the x_{trp} is shown as function of the integrated spectrum of L_p from 100 to 300 Hz for different AoA intervals.

For the AoA interval from 5 to 6 deg there is a clear tendency of earlier transition when the integral of P_{sp} increases. The same is found for the 7 to 8 deg interval while no real impact is seen on the 8 to 9 deg bin.

The 100 to 300 Hz interval is below the frequency interval of 500 to 7000 Hz that was used in computation of the amplification of the initial instabilities of the T-S waves for the wind tunnel experiment on the same airfoil section [12]. This indicates that the transition mechanism is different on the rotor and might be of the by-pass transition type.

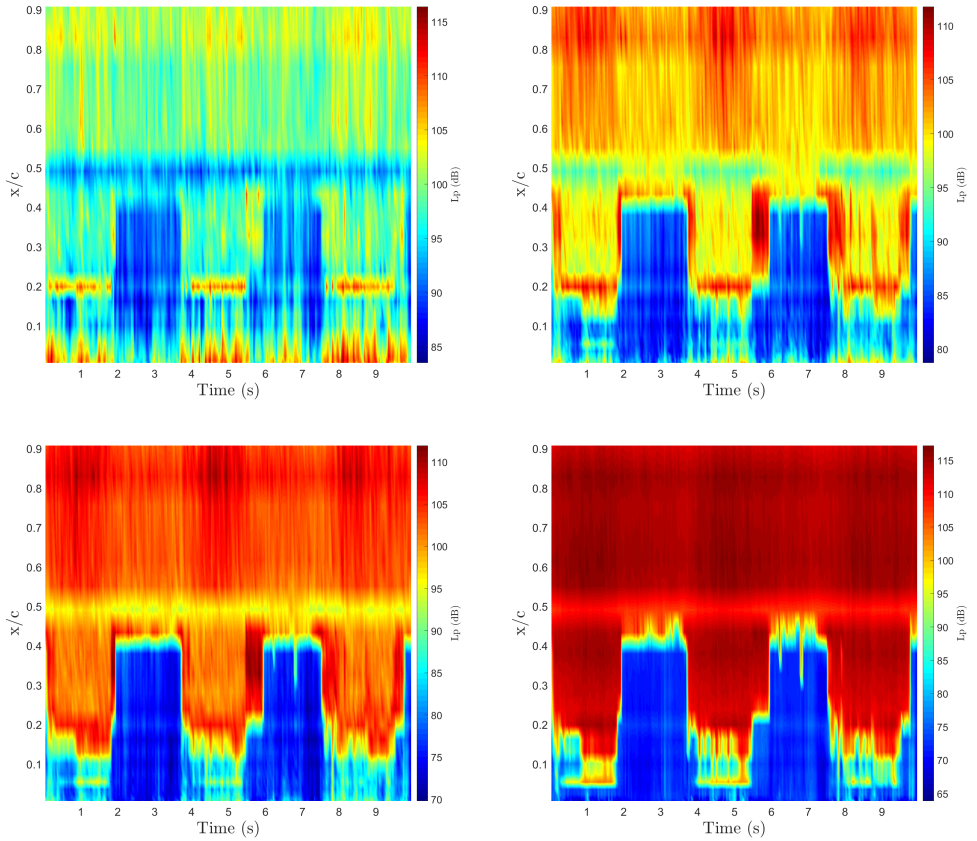

Fig. 10 Water fall plots of spectra of Lp on the pressure side for different frequency bands. Upper left 100-300Hz; Upper right; 300-600Hz; Lower left; 600-1000Hz and Lower right 2000-7000Hz. One of the wake cases.

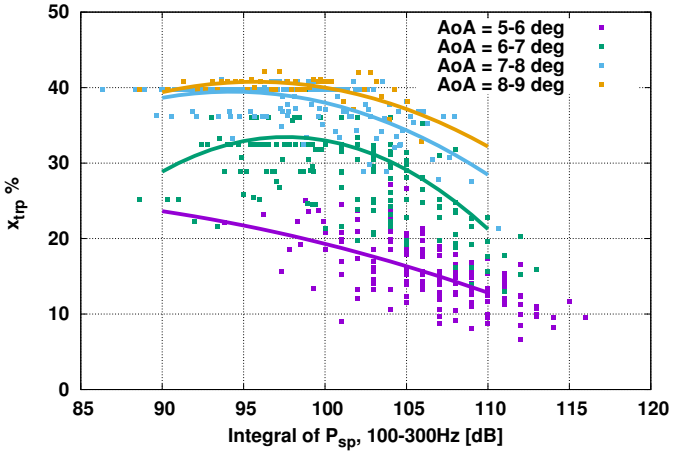

Fig. 11 The transition on the pressure side shown as function of the integral of P_{sp} over a frequency interval from 100-300 Hz for different $AoA's$.

VI. Conclusion

We presented a study with the objective to explore the fundamental differences in transition characteristics on a blade section in wind tunnel flow and on the blade of a full scale rotor (in the present case a 2MW turbine with an 80 m rotor). Flush mounted surface microphones are chosen as basis for the transition detection as it was found to be a robust method that would work on a turbine with atmospheric inflow.

The experiments confirm that the microphone installation work well. We develop and present a transition detection procedure based on monitoring the increase in spectral energy of the microphone signals in the frequency interval from 2000 to 7000 Hz.

When comparing the transition on a 2D blade section copy of the full-scale rotor blade section we find a much earlier transition on the rotor on the pressure side. On the suction side the difference is small probably due to an early transition in both the wind tunnel and the rotor case due to small bumps on the blade surface.

We also study the differences in inflow based on spectra of boundary pressure fluctuations in the laminar boundary layer close to the LE. It is found that below 300 Hz the inflow to the blade section on the rotor has a much higher energy content compared with the wind tunnel flow. However, above 300 Hz they are comparable with a tendency of slightly higher levels in the wind tunnel flow.

Finally, we show that there seems to be a correlation between increase in the 100-300 Hz energy content and the transition moving closer to the LE indicating a by-pass transition mechanism.

Acknowledgments

The present work is based on data from the DanAero MW project funded by the Danish Energy Research programme EFP-2007 under contract Journal nr.: 33033-0074. The project was carried out in the period from March 2007 to December 2009 in corporation between Risø DTU and the companies LM Glasfiber, Vestas Wind Systems, Siemens Wind Power and DONG Energy.

The project was followed by the "DANAERO MW II: Influence of atmospheric and wake turbulence on MW turbine performance, loading and stability" where the DanAero data base was established. This project was partly funded funded by EUDP2009-II and partly funded by the project partners (Vestas Wind Systems, LM Wind Power, Siemens Wind Power, DTU Wind Energy) themselves.

References

[1] VanIngen, "A Suggested Semi-Empirical Method for the Calculation of the boundary Layer Region," Tech. rep., Dept. Aerospace Eng., Techn. Univ. Holland, TR VTH71, VTH74, Delft, Holland, 1956.

[2] Sørensen, N. N., "CFD modelling of laminar-turbulent transition for airfoils and rotors using the gamma-(Re)over-tilde (theta) model," *Wind Energy*, Vol. 12, No. 8, 2009, pp. 715–733. doi:10.1002/we.325.

[3] Morkovin, M. V., "BYPASS TRANSITION TO TURBULENCE AND RESEARCH DESIDERATA," *Nasa Conference Publication*, 1985, pp. 161–211.

[4] Horstmann, K. H., Quast, A., and Redeker, G., "Flight and wind-tunnel investigations on boundary-layer transition," *Journal of Aircraft*, Vol. 27, No. 2, 1990, pp. 146–150. doi:10.2514/3.45910.

[5] Madsen, H., Bak, C., Paulsen, U., Gaunaa, M., Sørensen, N., Fuglsang, P., Romblad, J., Olesen, N., Enevoldsen, P., Laursen, J., and Jensen, L., "The DANAERO MW Experiments," *AIAA 2010-645, 48th AIAA Aerospace Sciences Meeting and Exhibit, Orlando, Florida*, 2010.

[6] Madsen, H., Bak, C., Paulsen, U., Gaunaa, M., Fuglsang, P., Romblad, J., Olesen, N., Enevoldsen, P., Laursen, J., and Jensen, L., "The DAN-AERO MW Experiments Final report," Tech. Rep. Risø-R-1726(EN), Technical University of Denmark, 2010.

[7] Troldborg, N., Bak, C., Aagaard Madsen, H., and Skrzypinski, W. R., "DANAERO MW II: Final Report," Tech. Rep. DTU Wind Energy E-0027(EN), 2013.

[8] Schaffarczyk, A. P., Schwab, D., and Breuer, M., "Experimental detection of laminar-turbulent transition on a rotating wind turbine blade in the free atmosphere," *Wind Energy*, Vol. 20, No. 2, 2017, pp. 211–220. doi:10.1002/we.2001.

[9] Døssing, M., "High Frequency Microphone Measurements for Transition Detection on Airfoils," Tech. Rep. Risø-R-1645(EN), Risø-DTU, Roskilde, Denmark, 2008.

[10] Fuglsang, P., and Bak, C., "Development of the Risø wind turbine airfoils," *Wind Energy*, Vol. 7, 2004, pp. 145–162.

[11] Bak, C., Andersen, P., Madsen, H., Gaunaa, M., Fuglsang, P., and Bove, S., "Design and Verification of Airfoils Resistant to Surface Contamination and Turbulence Intensity," *AIAA 2008-7050, 26th AIAA Applied Aerodynamics Conference, 18 - 21 August 2008, Honolulu, Hawaii*, 2008.

[12] Özçakmak, S., Sørensen, N., Madsen, H., and Sørensen, J., "Laminar-Turbulent Transition Detection on Airfoils by High Frequency Microphone Measurements," *Submitted for Wind Energy*, 2018.

[13] Døssing, M., Madsen, H., Bak, C., Fischer, A., Troldborg, N., Hansen, P., and F., B., "High frequency microphone measurements for detection of transition on airfoils," Tech. Rep. Risø-I-3177(EN), Risø-DTU, Roskilde, Denmark, 2011.

[14] Juul Larsen, T., Melchior Hansen, A., and Risø National Lab., W. E. D., DTU, *How 2 HAWC2, the user's manual*, 2007.

[15] Bertagnolio, F., and of Denmark. Risø National Lab. for Sustainable Energy. Wind Energy Div., T. U., *NACA0015 measurements in LM wind tunnel and turbulence generated noise*, 2008.